Title
Conformal MnO2 Electrodeposition Onto Defect-Free Graphitic Carbons

Journal
Electrochemistry Communications, 13(590-2)

Author
Collins, Philip G

Publication Date
2011

Peer reviewed

Electrochemistry Communications 13 (2011) 590–592

Contents lists available at ScienceDirect

Electrochemistry Communications

journal homepage: www.elsevier.com/locate/elecom

Conformal MnO2 electrodeposition onto defect-free graphitic carbons

Israel Perez, Brad L. Corso, Vaikunth R. Khalap, Philip G. Collins *

Department of Physics and Astronomy, University of California Irvine, Irvine, CA 92697, United States

ARTICLE INFO

Article history:
Received 2 March 2011
Received in revised form 12 March 2011
Accepted 14 March 2011
Available online 22 March 2011

Keywords:
Hybrid materials
Composite nanostructure
Carbon nanotube
Nanoelectrode

ABSTRACT

Uniform, conformal coating of MnO_2 onto single walled carbon nanotubes is achieved with precise thickness control and without the introduction or utilization of defect sites. The resulting composite electrodes enable electrochemical testing of novel carbon–metal oxide composites in which rate-enhancing, fast-electron-transfer defect sites are completely absent. Such sites are ubiquitous and believed to be enormously consequential to the electron transfer properties of graphitic carbon systems, and the techniques described here provide an experimental route to quantitatively study such effects. For example, we immediately discern the enhanced interfacial resistance that occurs in the defect-free system.

1. Introduction

The conductivity and chemical inertness of graphite is ideal for harsh electrochemical conditions, and this is why graphitic carbons are a key component material in a wide variety of electrochemical applications [1,2]. Often, the pristine carbon is merely a supporting substrate for a second material, such as catalytic metals [3] or charge storage oxides [4,5], or else the carbon itself is chemically attacked to enhance its chemical activity [6,7]. In each of these cases, interfacial charge transfer between the active layer and the graphitic support plays a critical role in the properties of the composite, but accurate characterization of the charge transfer rates is complicated by carbon defect sites. These sites are believed to have locally enhanced electron transfer kinetics that are one thousand-fold higher than that of the pristine, graphitic sp^2 lattice [8,9]. As a result, practical electrochemical properties end up dominated by highly inhomogeneous defect sites.

Remarkably, the exact contribution of defect sites is particularly difficult to determine experimentally. The highest quality graphitic systems, including highly-oriented pyrolytic graphite (HOPG), single layer graphene, and single walled carbon nanotube (SWNT) films, all contain defects at basal plane edges, grain boundaries, and SWNT ends. All graphitic electrodes are necessarily an ensemble of highly active but poorly characterized defects, intermixed in very low activity basal plane carbon. This issue is directly addressed in the recent review article by McCreery [1], noting that without precise control over the concentration and chemistry of the dominant defect sites, it is impossible to quantitatively determine fundamental electron transfer rates, either of the basal plane or of the defect sites.

To overcome this limitation and characterize the true interfacial properties of pristine graphitic carbon, we consider electrochemical working electrodes composed of one single SWNT. Previous work has demonstrated the feasibility of cyclic voltammetry on individual SWNTs [10–12], as well as the ability of SWNTs to transduce molecular electrochemistry [13,14]. Here, we apply these advantageous abilities to SWNT electrodes having more complex behaviors. Furthermore, we focus on high quality SWNTs having a protective coating over the endcaps, so that the system is wholly pristine, edge-free, and defect-free carbon. Starting in this state, a wide range of composite electrode types can be interrogated deterministically and quantitatively, for example by depositing other materials onto the carbon or introducing carbon defects.

The primary element of a SWNT electrochemical electrode is the electrically connected SWNT itself. The fabrication of these elements as transistors, chemical sensors, and other electrical elements has become quite common and various effective fabrication techniques exist. By comparison, a major hurdle to achieving the composite electrodes of interest is successful coating of the defect-free carbon. In the same manner that they dominate electron transfer properties, edges and defects serve as nucleation sites for most chemical, physical, and electrochemical deposition processes. So, for example, it is straightforward to electrochemically decorate just the step edges of HOPG [15,16], the defect sites on a SWNT [17], or chemically-etched nanotube materials [18–20]. It is much more difficult to uniformly and conformally coat defect-free carbon that lacks chemically active nucleation sites [21]. Sputtering, anodic deposition, atomic layer deposition, and many other techniques proceed by first introducing sp^3 lattice defects, but the unintentional introduction of such sites eliminates any advantage of the SWNT electrode proposed here.

* Corresponding author.
E-mail address: collinsp@uci.edu (P.G. Collins).

1388-2481/$ – see front matter © 2011 Elsevier B.V. All rights reserved.
doi:10.1016/j.elecom.2011.03.017

Instead, we have developed a bipotential, anodic electrodeposition scheme for producing uniform metal oxide coatings onto SWNTs that can be accomplished without introducing defects. In this letter, we focus on a SWNT–MnO_2 heterostructure, a particular composite of interest in electrochemical capacitor and Li ion battery research and applications [22,23]. The technique, however, is readily generalizable to various metal oxides.

2. Experimental methods

Our SWNTs are grown using high temperature (940 °C), plasma-free chemical vapor deposition to achieve long, straight, and defect-free SWNT segments. The catalyst for growth is FeMo nanoparticles diluted in ethanol (<1:1000 by vol) and spun onto a Si/SiO_2 wafer to give isolated, small diameter (1.2 ± 0.2 nm) SWNTs.[24] SWNT segments are then lithographically contacted by Pt electrodes [24,25]. On top of the fabricated devices, electron beam resist (PMMA) is applied and patterned so as to expose ≤ 1 μm of the SWNT sidewall to electrolytes, while providing a protective coating to the rest of the SWNT, the Pt electrodes, and the SWNT–Pt contact interfaces. We note that capping the initial Pt metal with Ti is quite effective at reducing electrochemical leakage currents that can arise from PMMA pinholes or surface debris.

Anodic deposition of MnO_2 from 10 mM manganese acetate is performed both with and without a supporting electrolyte of 250 mM lithium perchlorate ($LiClO_4$, aq.). Depositions on SWNTs are characterized by atomic force and scanning electron microscopy, and cyclic voltammetry in $LiClO_4$. Similar depositions on HOPG provide large area films for comparison and x-ray diffraction analysis.

To obtain uniform coatings on defect-free carbon, a two-step scheme (Fig. 1a) has been developed that is similar to edge- and defect-selective deposition techniques for HOPG and SWNTs [15–17]. First, a nucleation pulse at potential $V_{nuc} = 1.0$ V (vs. Pt) is applied for 10 ms to seed a uniform distribution of nuclei along the exposed surface. Immediately after, deposition is driven at a much lower potential V_{dep}. The magnitude of V_{nuc} is selected to be just below the threshold for nucleating covalent adducts to the carbon lattice [25]. While $V_{nuc} = 1.0$ V is suitable for most aqueous reagents, this potential can introduce covalent defects in acidic solutions or strong oxidants [25]. In those cases, lower V_{nuc} values of 0.8–0.9 V are required in order to maintain the uniformity of the desired nucleation layer and the quality of the underlying carbon support.

3. Results and discussion

Fig. 1 compares MnO_2 depositions achieved at $V_{dep} = 0.1$ V with and without V_{nuc}, and clearly illustrates the advantage of the initial nucleation pulse in achieving uniform coatings. When the nucleation technique is used, uniform and conformal coatings are routinely obtained.

Following this enabling initial nucleation, the subsequent electrochemical deposition can be very finely controlled. Fig. 2 shows MnO_2 deposition thicknesses achieved on SWNTs at $V_{dep} = 0.1$ V for different durations, in order to calibrate the deposition rate at this potential. In 10 mM manganese acetate, the average deposition rate is 1.3 nm/s. With the addition of $LiClO_4$ supporting electrolyte, the deposition rate doubles to 2.5 nm/s and likely produces a lithiated $LiMnO_2$ [26]. Both deposition rates are low enough to allow precise control of MnO_2 film thickness, a specific advantage of working at low V_{dep}. In fact, the initial V_{nuc} pulse enables highly controlled growth over a wide range of V_{dep} values and electrolyte concentrations, the combination of which are critical to both final morphology and material performance. Thus, for example, we achieve continuous coatings produced at very low potentials ($V_{dep} < 0.3$ V) where deposition is usually highly nonuniform and characterized by random, dilute nucleation and diffusion-limited blooming at isolated sites or along step edges [16]. Film thickness is believed to be a critical parameter in MnO_2 applications [27], in part because the low conductivity of MnO_2 limits its pseudocapacitive performance. Both thickness and composition can be completely controlled by V_{dep} when the nucleation technique described here is used.

The linear fits in Fig. 2 have nonzero intercepts of 7–9 nm. At zero V_{dep} duration, this film thickness is entirely due to the initial coating that occurs during the nucleation pulse. Lower V_{nuc} values can reduce the thickness of this seed layer, but they can also compromise the film uniformity. Higher V_{nuc} values introduce point defects into the SWNT lattice, as evidenced by concurrent conductivity measurements. In fact, the particular advantage of SWNTs over two-dimensional HOPG or graphene is precisely their one-dimensional conductivity and sensitivity to induced damage at the single defect limit [25]. None of the SWNT devices coated in Fig. 2 exhibit conductance changes that would indicate the presence of oxidative damage.

After fabrication, successful electrochemical testing of these composite electrodes is a measurement challenge, though any low noise, high gain (10^{10} V/A) configuration is usually sufficient. We probe SWNT–MnO_2 devices by cyclic voltammetry in 250 mM $LiClO_4$,

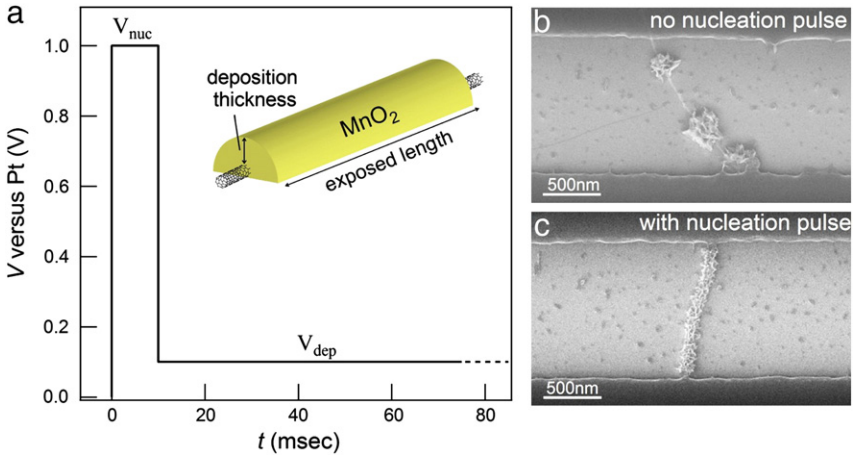

Fig. 1. (a) Bipotential deposition scheme involves a nucleation pulse (V_{nuc}) 10 ms in duration, followed by deposition at much lower potential (V_{dep}). MnO_2 electrodeposition for 60 s poorly coats pristine SWNTs without any nucleation (b), but under the same conditions results in a conformal coating when preceded by the nucleation pulse (c). In both images, the SWNT extends under a protective PMMA coating to its electrical contact with Pt electrodes.

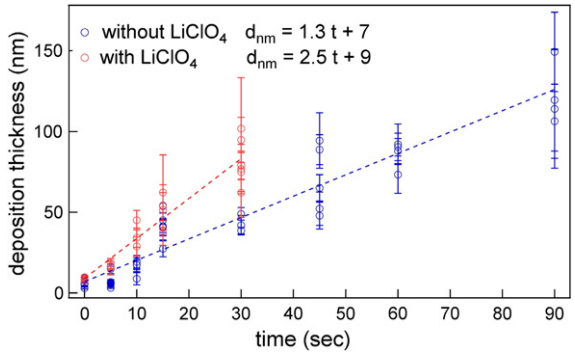

Fig. 2. Deposition thickness vs. V_{dep} duration in 10 mM manganese acetate with (circles) and without (triangles) supporting electrolyte of 250 mM $LiClO_4$. Each data point represents a single SWNT device characterized by AFM, with error bars representing the film thickness variability along the SWNT axis. Linear fits (dashed lines) suggest kinetically-controlled deposition at rates specified.

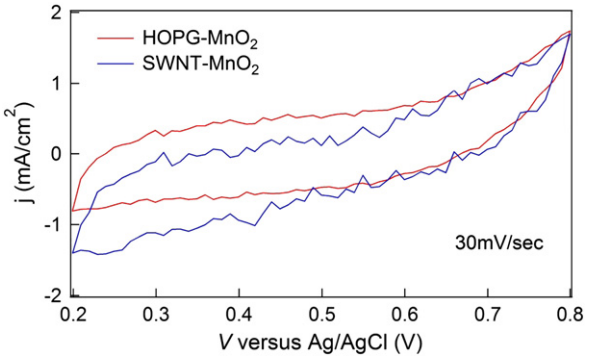

Fig. 3. Cyclic voltammetry (CV) of a SWNT–MnO_2 device compared to the CV of a similarly deposited HOPG–MnO_2 electrode. CVs from HOPG electrodes approach the ideal, rectangular shape for reversible charge/discharge kinetics. CVs are done in 250 mM $LiClO_4$ at a scan rate of 30 mV/s. Current density data is normalized to carbon electrode area.

in order to observe Li^+ charging and discharging. At a scan rate of 30 mV/s, the charging current exceeds 1 pA for a device like the one shown in Fig. 1c. This magnitude of current, albeit small, is easily distinguished above our typical peak-to-peak noise level of 20 fA (achieved using a Keithley model 428 current preamplifier).

Fig. 3 compares cyclic voltammograms (CVs) of a composite SWNT–MnO_2 device and a similarly prepared microelectrode of HOPG–MnO_2. This pair of systems highlights the motivation of fabricating the former: the SWNT carbon is defect-free, while the HOPG has a low but pertinent density of step edges and point defects. The exposed HOPG sample area is limited by electron beam lithography to an active surface area of 1.4×10^9 nm^2, whereas the SWNT–MnO_2 electrode has a surface area of 9400 nm^2. Despite the disparity, Fig. 3 demonstrates that the CVs have very similar charge–discharge characteristics once normalized by electrode area. In fact, the direct comparison between such similar electrodes establishes the presence of a slight difference in kinetics between the two cases. Although quantitative analysis is outside the scope of this letter, the SWNT device in Fig. 3 has a slanted CV compared to the HOPG device, possibly indicating the effects of higher series resistance across the more pristine carbon interface. The two distinct charging kinetics in Fig. 3 motivate further study of the defect-free carbon system.

4. Conclusions

In conclusion, we have developed a technique for coating pristine SWNTs with electrodeposited metal oxides like MnO_2. A nucleation technique enables the deposition of uniform, continuous MnO_2 films using a wide range of the deposition potentials or electrolyte concentrations. The device conductances establish that the underlying SWNTs remain defect-free, permitting precise investigation of the role of such defects in electrochemical interfacial properties. A modest decrease is already noted between MnO_2 deposited on defective HOPG and on defect-free SWNTs. Similar devices with MnO_2 or other pseudocapacitive materials should help inform the optimization of carbon electrode chemistries, especially for larger area composite electrodes using graphenes and other graphitic carbons.

Acknowledgements

We thank W. Yan and R. Penner for discussion and sharing the results of synergetic experiments. This research was supported by NSF (CBET-0729630) and the NEES Energy Frontier Research Center of the U.S. DOE Office of Basic Energy Sciences (#DESC0001160).

References

[1] R.L. McCreery, Chem. Rev. 108 (2008) 2646.
[2] L.L. Zhang, R. Zhou, X.S. Zhao, J. Mater. Chem. 20 (2010) 5983.
[3] G.G. Wildgoose, C.E. Banks, R.G. Compton, Small 2 (2006) 182.
[4] D.R. Rolison, R.W. Long, J.C. Lytle, A.E. Fischer, et al., Chem. Soc. Rev. 38 (2009) 226.
[5] R. Liu, J. Duay, S.B. Lee, Chem. Commun. 47 (2011) 1384.
[6] L.J. Fu, H. Liu, C. Li, Y.P. Wu, et al., Solid State Sci. 8 (2006) 113.
[7] M. Pumera, T. Sasaki, H. Iwai, Chem. Asian J. 3 (2008) 2046.
[8] T.J. Davies, R.R. Moore, C.E. Banks, R.G. Compton, J. Electroanal. Chem. 574 (2004) 123.
[9] K.R. Kneten, R.L. McCreery, Anal. Chem. 64 (1992) 2518.
[10] I. Heller, J. Kong, H.A. Heering, K.A. Williams, et al., Nano Lett. 5 (2005) 137.
[11] T.M. Day, N.R. Wilson, J.V. Macpherson, J. Am. Chem. Soc. 126 (2004) 16724.
[12] J. Kim, H. Xiong, M. Hofmann, J. Kong, et al., Anal. Chem. 82 (2010) 1605.
[13] B.R. Goldsmith, J.G. Coroneus, A.A. Kane, G.A. Weiss, et al., Nano Lett. 8 (2008) 189.
[14] H. Shen, W.L. Xu, P. Chen, Phys. Chem. Chem. Phys. 12 (2010) 6555.
[15] Q.G. Li, J.B. Olson, R.M. Penner, Chem. Mater. 16 (2004) 3402.
[16] M.P. Zach, K. Inazu, K.H. Ng, J.C. Hemminger, et al., Chem. Mater. 14 (2002) 3206.
[17] Y.W. Fan, B.R. Goldsmith, P.G. Collins, Nat. Mater. 4 (2005) 906.
[18] Y. Shan, L. Gao, Chem. Lett. 33 (2004) 1560.
[19] L. Fu, Z.M. Liu, Y.Q. Liu, B.X. Han, et al., Adv. Mater. 16 (2004) 350.
[20] K. Balasubramanian, M. Burghard, J. Mater. Chem. 18 (2008) 3071.
[21] T.M. Day, P.R. Unwin, J.V. Macpherson, Nano Lett. 7 (2007) 51.
[22] C. Liu, F. Li, L.P. Ma, H.M. Cheng, Adv. Mater. 22 (2010) E28.
[23] C. Jinhua, F. Zhen, W. Mingyong, K. Cui, et al., Diamond Relat. Mater. 15 (2006) 1478.
[24] L. An, J.M. Owens, L.E. McNeil, J. Liu, J. Am. Chem. Soc. 124 (2002) 13688.
[25] B.R. Goldsmith, J.G. Coroneus, V.R. Khalap, A.A. Kane, et al., Science 315 (2007) 77.
[26] M. Nakayama, T. Kanaya, J.W. Lee, B.N. Popov, J. Power Sources 179 (2008) 361.
[27] C.J. Xu, F.Y. Kang, B.H. Li, H.D. Du, J. Mat. Res. 25 (2010) 1421.